Novel Phenomena in Very-Low-Frequency Strong Fields

H. R. Reiss

Max Born Institute, 12489 Berlin, Germany and American University, Washington, D.C. 20016-8058, USA

(Received 17 December 2008; published 9 April 2009)

Atomic ionization by lasers of very low frequency, once thought to be a classical limit or a "tunneling limit", presents unique spectral features unlike any tunneling phenomenon. The identity of the atom is the controlling factor, leading to photoelectron spectra with well-defined peaks and valleys that persist over wide ranges of field parameters. Such a spectrum was observed 20 years ago in ionization of xenon at 10.6 μm.

DOI: 10.1103/PhysRevLett.102.143003 PACS numbers: 32.80.Rm, 32.90.+a, 42.50.Hz

It was demonstrated recently [1] that atomic ionization by strong-field lasers is subject to limitations on the applicability of tunneling theories, particularly in the existence of a low-frequency limit in addition to the universally recognized high-frequency limit. It is natural to inquire about how low-frequency behavior would reveal itself in laboratory experiments. There has been an answer to this question in the literature for 20 years. Photoionization of xenon by a CO_2 laser operating at 10.6 μm and about 10^{14} W/cm^2 was found to have a photoelectron spectrum with seemingly inexplicable features [2]. One is a prominent peak at a low energy that is nonetheless clearly separated from zero energy, and another is a broad but plainly visible peak occurring at an energy in excess of 100 eV. These features can be seen in Fig. 1, taken from Ref. [2]. The conditions of the experiment are such that it remains nonrelativistic.

It is shown below that precisely such features are displayed in a velocity-gauge theory of strong-field ionization, even when a dipole-approximation theory is employed, whereas a tunneling theory of strong-field ionization possesses no mechanism to explain this double-peaked behavior of the spectrum.

The expectation from a tunneling theory had been that an experiment at such a long wavelength as 10.6 μm would provide access to the classical limit (also called the tunneling limit) of strong-field phenomena (see, for example, Ref. [3]), based on the approach to a zero value of the Keldysh parameter

$$\gamma = \sqrt{\frac{E_B}{2U_p}} = \frac{\omega}{I^{1/2}}\sqrt{2E_B}, \tag{1}$$

where E_B is the field-free binding energy of the initially bound electron, and U_p is the ponderomotive energy of the ionized electron due to its interaction with the laser field of frequency ω and intensity I. Atomic units are used in this paper unless otherwise specified. The expectation of a low-frequency approach to a classical limit is contradicted experimentally by the Université de Laval results [2], as well as theoretically by the demonstration [1] that the putative "tunneling limit" is nonexistent. Even if the tunneling concept is abandoned, there remains the need to explain the persistence of these unusual spectral qualities in the face of the smoothing effects due to averaging over the broad range of intensities that exist in a laser beam of Gaussian time profile brought to a Gaussian focus.

It is the conclusion of this present work that the qualities of the spectrum observed [2] by the Université de Laval

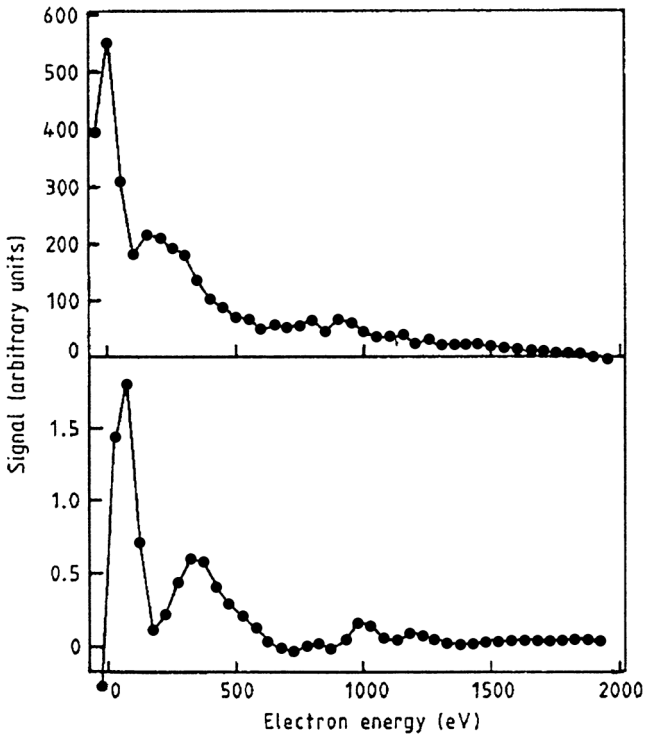

FIG. 1. This is a reproduction of a figure from Ref. [2], showing the photoelectron spectrum from the ionization of ground-state xenon by a CO_2 laser operating at 10.6 μm. Although the data were not abundant, they were still sufficient to allow a spectrum to be generated that shows the presence of two prominent peaks.

group are indeed representative of the special properties possessed by ionization caused by strong-field lasers of very low frequency.

The intensity parameters of the Laval experiment with the CO_2 laser are informative. There are three dimensionless parameters z, z_1, z_f that can be formed from ratios of the four energies U_p, ω, E_B, mc^2 characteristic of strong-field ionization:

$$z \equiv U_p/\omega = 9000, \qquad z_1 \equiv 2U_p/E_B = 173, \qquad z_f \equiv 2U_p/mc^2 = 0.004, \tag{2}$$

where the electron mass m has been retained to preserve the recognizability of the electron rest energy mc^2 even though $m = 1$ in atomic units. The numerical values are those of the Laval experiment. The parameter z is a measure of the applicability of perturbation theory [4,5]. For the process to be perturbative, $z \ll 1$ is necessary, so perturbation theory can offer no guidance here. Also, z represents the number of photons required to allow the free electron to be a physical particle in the presence of the field. The experiments were of very low frequency, but they were nevertheless not classical. The z_1 parameter measures the extent to which effects of the laser field dominate residual Coulomb effects on the photoelectron. The strong-field approximation (SFA) [4,5] requires $z_1 \gg 1$, which is amply satisfied. Equations (1) and (2) show the connection $z_1 = 1/\gamma^2$. The z_f parameter is an indicator of the significance of relativistic effects, which are not important here.

The SFA [4,5] represents the laser field by a vector potential. Its usual form is in the dipole approximation. Nevertheless, it possesses a continuous connection to the fully Dirac-relativistic SFA [5–7], and the qualitative features unique to the very-low-frequency ionization domain are found to exist within the SFA even in the dipole approximation. Despite the possibility of some numerical inadequacy, it is desirable to take advantage of the analytical clarity of the dipole-approximation SFA.

General properties of the SFA transition probability expression serve to explain the novel features of very-low-frequency ionization. For linearly polarized laser fields, the SFA differential total transition rate is

$$\frac{dW}{d\Omega} = \frac{1}{(2\pi)^2} \sum_{n=n_0}^{\infty} p\left(\frac{p^2}{2} + E_B\right)^2 \times |\phi_i(p)|^2 [J_n(\alpha_0 p\cos\theta, -\beta_0 c)]^2, \quad \text{where} \tag{3}$$

$$n_0 \geq \frac{1}{\omega}(E_B + U_p), \qquad \phi_i(p) = \int d^3r \exp(-i\mathbf{p}\cdot\mathbf{r})\phi_i(\mathbf{r}), \tag{4}$$

$$\alpha_0 = \frac{c}{\omega}\sqrt{\frac{2z_f}{1+z_f}} \approx 2\sqrt{\frac{z}{\omega}}, \qquad \beta_0 = \frac{c}{\omega}\frac{z_f}{4(1+z_f)} \approx \frac{cz_f}{4\omega}, \tag{5}$$

$$\frac{p^2}{2} = n\omega - E_B - U_p. \tag{6}$$

Here, $\phi_i(p)$ is the momentum-space wave function corresponding to $\phi_i(\mathbf{r})$, which is the space part of the stationary-state wave function of the noninteracting initial state; α_0 is the amplitude of the excursion in the polarization direction of a free electron in the laser field, β_0 is the corresponding amplitude in the field propagation direction; and θ is the polar angle of spherical coordinates with respect to an axis in the polarization direction. The functions J_n with two arguments are the generalized Bessel functions [4,8]. The n-dependent energy conservation condition in Eq. (6) comes from the energy delta function associated with each of the terms in the sum over n, suggesting a photon order interpretation for the index n.

An important property of the transition rate in Eq. (3) is that the first three factors are expressed entirely in terms of the kinetic momentum p, and thus they are universal features of energy spectra of the atom. That is, a momentum factor $F(p)$ can be defined as

$$F(p) \equiv p\left(\frac{p^2}{2} + E_B\right)^2 |\phi_i(p)|^2, \tag{7}$$

that will characterize all photoelectron energy spectra arising from the initial-state atom identified by $\phi_i(\mathbf{r})$. The multiplicative factor p, the first factor to the left in Eq. (7), will generally cause a minimum at the beginning of an energy spectrum produced by linearly polarized light. This then means that there will be a maximum occurring at a low energy [9]. Equation (7) also includes a different mechanism, arising from $|\phi_i(p)|^2$, that is responsible for structure in a photoelectron spectrum produced by linearly polarized light.

Figure 2 shows $F(p)$ calculated using analytical Hartree-Fock representations [10] for $\phi_i(\mathbf{r})$, that are then analytically transformed to $\phi_i(p)$ in accordance with Eq. (4). Part (d) of Fig. 2 is for xenon, which was used in the Laval experiment, and the other parts of the figure show the other noble gases that have initial angular momentum $l = 1$ states.

The rate $dW/d\Omega$ comes from $F(p)$ modulated by the square of the generalized Bessel function $J_n(u, v)$. This function arises from the Volkov solution used in the SFA to describe the ionized electron, and coupling to atomic parameters exists because of the energy conservation condition in Eq. (6). Although $F(p)$ is a universal factor in all spectra arising from a given atom, this universality is usually obscured by the great variability of the $[J_n(u, v)]^2$ modulation. Figure 3(a) shows $[J_n(u, v)]^2$ at a wavelength of 800 nm for E_B corresponding to xenon,

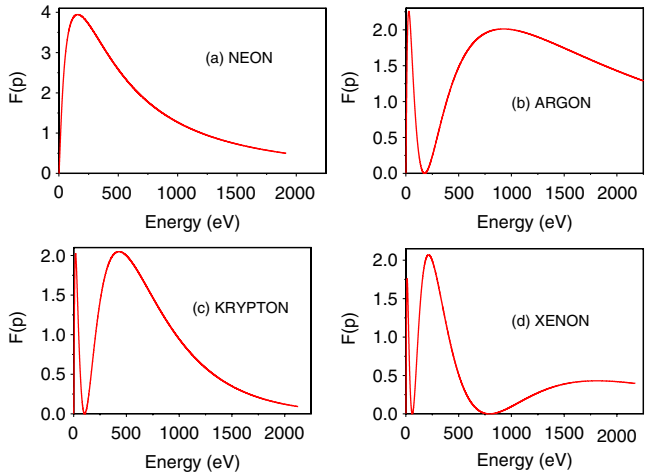

FIG. 2 (color online). The momentum-dependent function $F(p)$ defined in Eq. (7) is shown for the noble gases that possess initial p states. The $F(p)$ for argon, krypton, and xenon have a sharp peak at low energy. The exact location is difficult to discern in this figure, but the first peak occurs at about 12 eV for xenon, 18 eV for krypton, and 27 eV for argon.

showing the major effects of slight variations in the field intensity. It is clear that the universality of the $F(p)$ quantity is completely masked by the necessary integration over all the intensities that exist in the spatiotemporal profile of intensity in the laser focus. Major variability in $[J_n(u, v)]^2$ also arises as a function of the angle θ that exists in the first argument, u.

In contrast to the behavior described for 800 nm, Fig. 3(b) shows $[J_n(u, v)]^2$ for 10.6 μm, plotted as a function of energy. The figure is for xenon, but the extremely rapid fluctuation within a smoothly declining envelope holds true for any E_B. It is now clear that it is possible for the universal character of $F(p)$ to manifest itself, as shown in Fig. 4(a), giving the product of $F(p)$ and

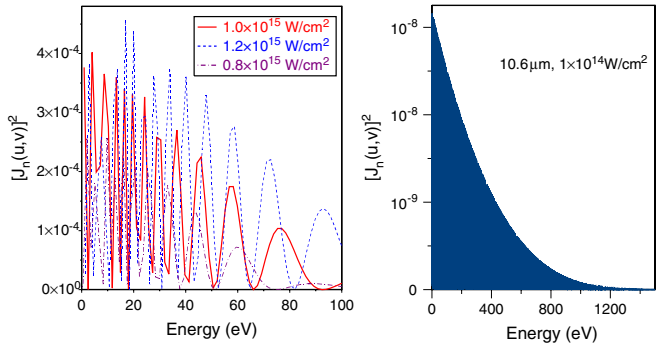

FIG. 3 (color online). The square of the generalized Bessel function modulates the $F(p)$ given in Fig. 2. (a) At 800 nm, small differences in intensity cause major changes in this modulation. The result is that the spatiotemporal distribution of intensity in the laser focus will mask the basic $F(p)$ form. (b) In contrast to the case of 800 nm in (a), the squared generalized Bessel function at 10.6 μm possesses a smoothly decreasing envelope.

$[J_n(u, v)]^2$ for the 10.6 μm wavelength. The effect of the $[J_n(u, v)]^2$ modulation is simply to change the relative amplitudes of the peaks in $F(p)$. (Note that the energy scale in Fig. 2 is more extensive than in any part of Fig. 4.)

The universality of $F(p)$ preserves the basic location of the spectral peaks even in the presence of the major changes in intensity within the spatial and temporal distributions that occur in the laser focus. Figure 4(b) gives the spectrum for xenon ionized by 10.6 μm radiation in the Gaussian focal region and Gaussian temporal variation that existed in the Laval experiments. The proper way to incorporate S-matrix information in a spatiotemporal distri-

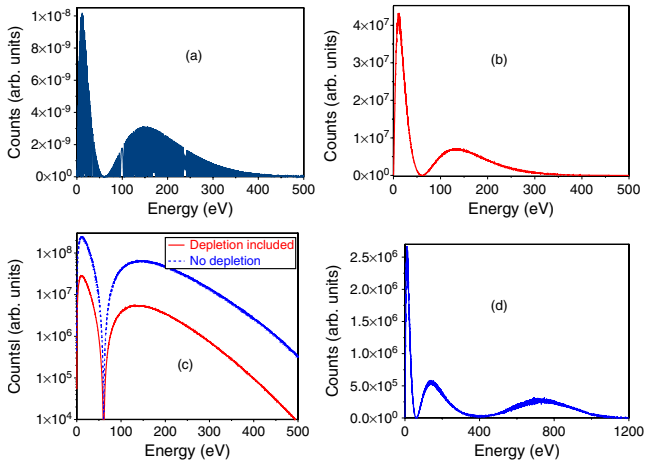

FIG. 4 (color online). (a) This figure shows the product of the $F(p)$ function for xenon in Fig. 2(d) and the $[J_n(u, v)]^2$ envelope function for 10.6 μm in Fig. 3(b). The result amounts to an isointensity spectrum for xenon at 10.6 μm. The peak structure of Fig. 2(d) is retained, but with the relative peak amplitudes altered because of the decline of the envelope function. The localized gaps in Fig. 3(b) remain. The locations of these gaps have an intensity dependence that minimizes their effect when integrated over the spatiotemporal focal profile of the laser. The fundamental peak structure of the $F(p)$ for xenon is preserved. (b) In this figure, the spectrum obtained from a full treatment of the laser focal intensity profile is presented, including the effects of saturation. The basic $F(p)$ structure is maintained. The considerable depletion effects that are a consequence of the very long pulse length do not appreciably shift the locations of the peaks. The peak at 12 eV for xenon in Fig. 2(d) has been shifted to about 10 eV. (c) This figure is related to (b), except it is plotted on a logarithmic scale to make possible a comparison of spectra with and without depletion effects. The consequences of depletion for location of the peaks are minor. (d) An approximate correction for the effects of ponderomotive energy recovery from the long pulse is applied in this figure. See the text for further explanation. The two main xenon peaks remain, but an additional higher-energy peak appears in consequence of the recovery of ponderomotive energy. The maximum value of U_p in the laser pulse is about 1 keV. This is responsible for shifting the far end of the spectrum to a higher energy, although the shift is less than the full $(U_p)_{\max}$. [The energy axis in (d) is more extensive than in (a)–(c).]

bution of intensities is to employ it as the local rate within the solution of a rate equation, as described in Refs. [5,9]. It is thus a simple matter to incorporate fully the effects of saturation within the laser focus. Figure 4(c), which displays the consequences of depletion of the neutral atoms, still maintains the peaks in the spectrum shown in Fig. 4(a). (A logarithmic vertical axis is used in Fig. 4(c) to make both the no-depletion and the with-depletion curves simultaneously visible.) The resemblance of the calculated spectrum in Fig. 4(b) to the experimental spectrum in Fig. 1 is clear.

The only matter still not accounted for is the recovery of ponderomotive energy that will occur within the very long pulses employed in the 1988 experiments [2]. This is a more complicated effect to calculate than are the results in Figs. 4(a)–4(c). An approximate technique has been employed to produce Fig. 4(d). The procedure used is not robust, and the results are presented only to show some qualitative features of ponderomotive energy recovery in a very long pulse. To explain the method, it is remarked that the extremely high photon orders necessary to achieve ionization at 10.6 μm, shown by the very large z value in Eq. (2), means that depletion takes a long time to develop. Saturation in the case of xenon becomes nearly complete after about 200 ps in the nanosecond pulse. (For the case of neon, for example, measurable ionization is produced, but saturation is never reached even within the full nanosecond of the pulse, in consequence of the relatively large binding energy that has to be supplied in neon.) The model used to estimate the recovery of U_p is to track each ionization event that occurs within the spatiotemporal profile of the pulse during that first 200 ps, assuming that the kinetic energy at the instant of ionization is maintained until the peak of the pulse at 500 ps. It is then assumed that the local (in space and time) ponderomotive energy that exists at the end of this track is the amount of ponderomotive energy that has been recovered by the end of the pulse. This means that some photoelectrons, those that occur near the edges of the spatial and temporal intensity variation, will escape from the focal region without significant ponderomotive energy recovery. The end result of this approximate procedure is shown in Fig. 4(d).

A striking feature of this final result is the preservation, almost unchanged, of the prominent low-energy peak in the spectrum, of the strong minimum that occurs at a slightly higher energy, and of the broad peak at about 150 eV that characterizes xenon. Beyond these features, the effect of ponderomotive energy recovery is to create an additional broad peak at several hundred eV, and to extend the tail of the distribution out to about 1 keV, rather than the initial 500 eV that occurs in Fig. 4(b).

(Note that the experimental spectrum in Fig. 1 is plotted on a graph that does not have its zero point at the lower-left extremity of the plot as it is in Figs. 2 through 4(d).)

In summary, very-low-frequency photoelectron spectra are qualitatively different from spectra familiar at shorter wavelengths. The velocity-gauge SFA analytical approximation is found to exhibit unusual spectral features that are identified as arising from the identity of the atom being ionized. It has also been shown why these spectral signatures do not arise at higher laser frequencies such as those associated with the familiar wavelengths in the neighborhood of 800 nm. The extremely high photon orders required for ionization do not signify an approach to classical conditions. Rather, they mean that the coupling to the laser field produces a rapid oscillation with a slowly declining envelope as a function of photoelectron energy. This property then reveals the underlying peak structure that characterizes the atom being ionized. These novel properties were actually observed in experiments performed 20 years ago.

It is also remarked that the ability of an analytical approximation to reveal all of these spectral features on an energy scale of the order of a keV is beyond the present capabilities of direct numerical integration of the time-dependent Schrödinger equation (TDSE), whose utilization was pioneered some years ago by Kulander [11], and by Javanainen, Eberly, and Su [12].

[1] H. R. Reiss, Phys. Rev. Lett. **101**, 043002 (2008).
[2] W. Xiong, F. Yergeau, S. L. Chin, and P. Lavigne, J. Phys. B **21**, L159 (1988).
[3] V. S. Popov, JETP Lett. **70**, 502 (1999).
[4] H. R. Reiss, Phys. Rev. A **22**, 1786 (1980).
[5] H. R. Reiss, Prog. Quantum Electron. **16**, 1 (1992).
[6] H. R. Reiss, J. Opt. Soc. Am. B **7**, 574 (1990).
[7] D. P. Crawford, Ph.D. Dissertation, American University, 1994.
[8] V. P. Krainov, H. R. Reiss, and B. M. Smirnov, *Radiative Processes in Atomic Physics* (Wiley, New York, 1997), Appendix J.
[9] H. R. Reiss, Phys. Rev. A **54**, R1765 (1996).
[10] A. A. Radzig and B. M. Smirnov, *Reference Data on Atoms, Molecules, and Ions* (Springer, Berlin, 1985).
[11] K. C. Kulander, Phys. Rev. A **35**, 445 (1987).
[12] J. Javanainen, J. H. Eberly, and Q. Su, Phys. Rev. A **38**, 3430 (1988).